

# Utilisation des codes PIC pour l'étude des interactions plasma-paroi à l'IJL

## Atelier Gaines Plasmas

Jérôme Moritz

Institut Jean Lamour - CNRS - Université de Lorraine. Campus Artem 2 allée André Guinier BP 50840  
54011 Nancy Cedex – France.

04/11/2024



# Outline

- A) Temperature of a tungsten surface under high heat flux plasma  
Thesis C. Djerroud (initiation of unipolar arcs started 2019)
- B) Erosion & redeposition of a liquid metal PFCs  
Thesis R. Avril / Renaissance Fusion (started 2023)
- C) Radio-frequency sheath and sputtering mitigation (ICRF antennas)  
Thesis L. Tsowemoo / IPP Garching – V. Bobkov (started 2024)

# A) Temperature of a tungsten surface under high heat flux plasma

→ J. Moritz et al, Nuclear Materials and Energy 41, 101753 (2024)

→ J. Moritz et al, Phys. Plasmas 30, 083514 (2023)

# Experimental context of bifurcation

Ye et al. / J Nucl. Mat. 241, 1243 (1997)

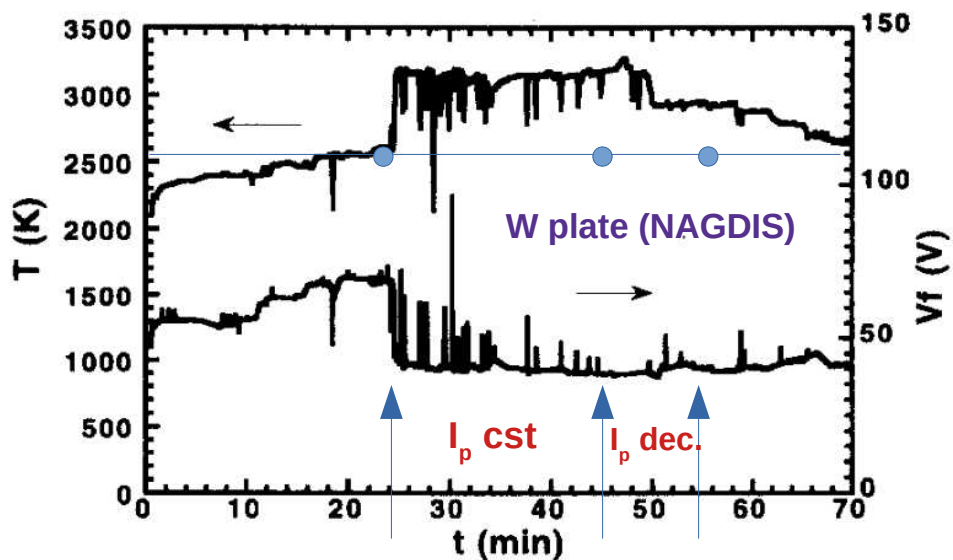
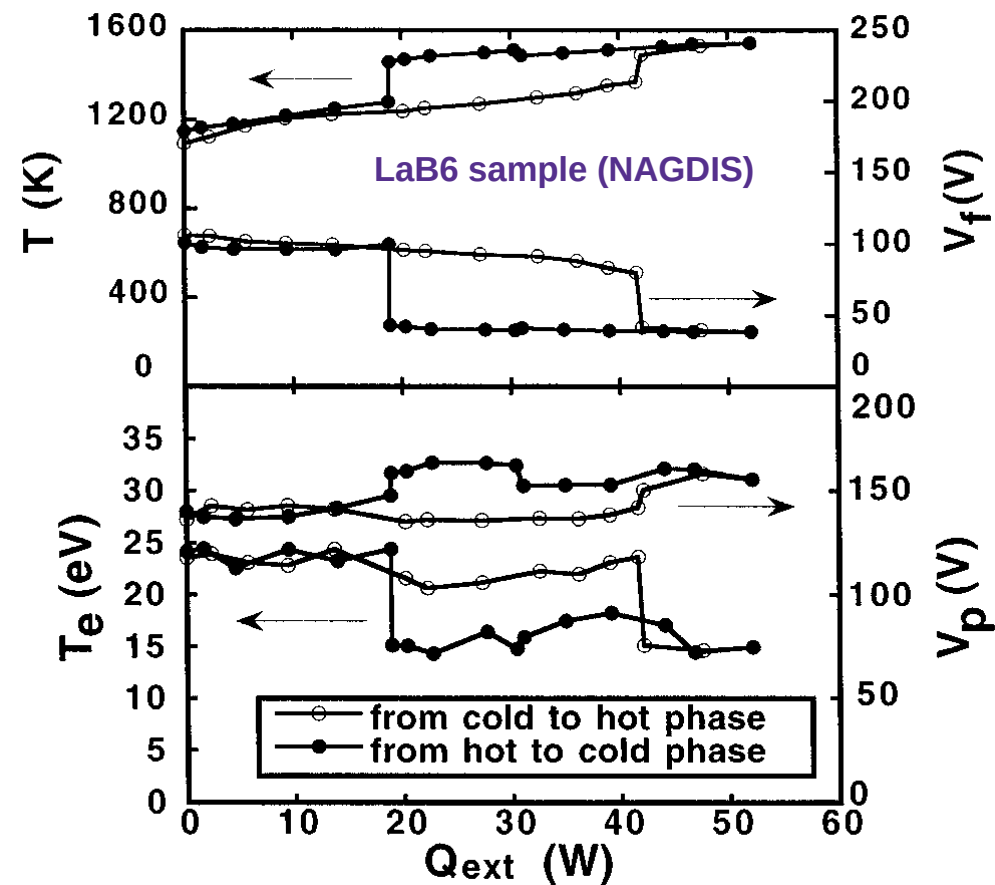


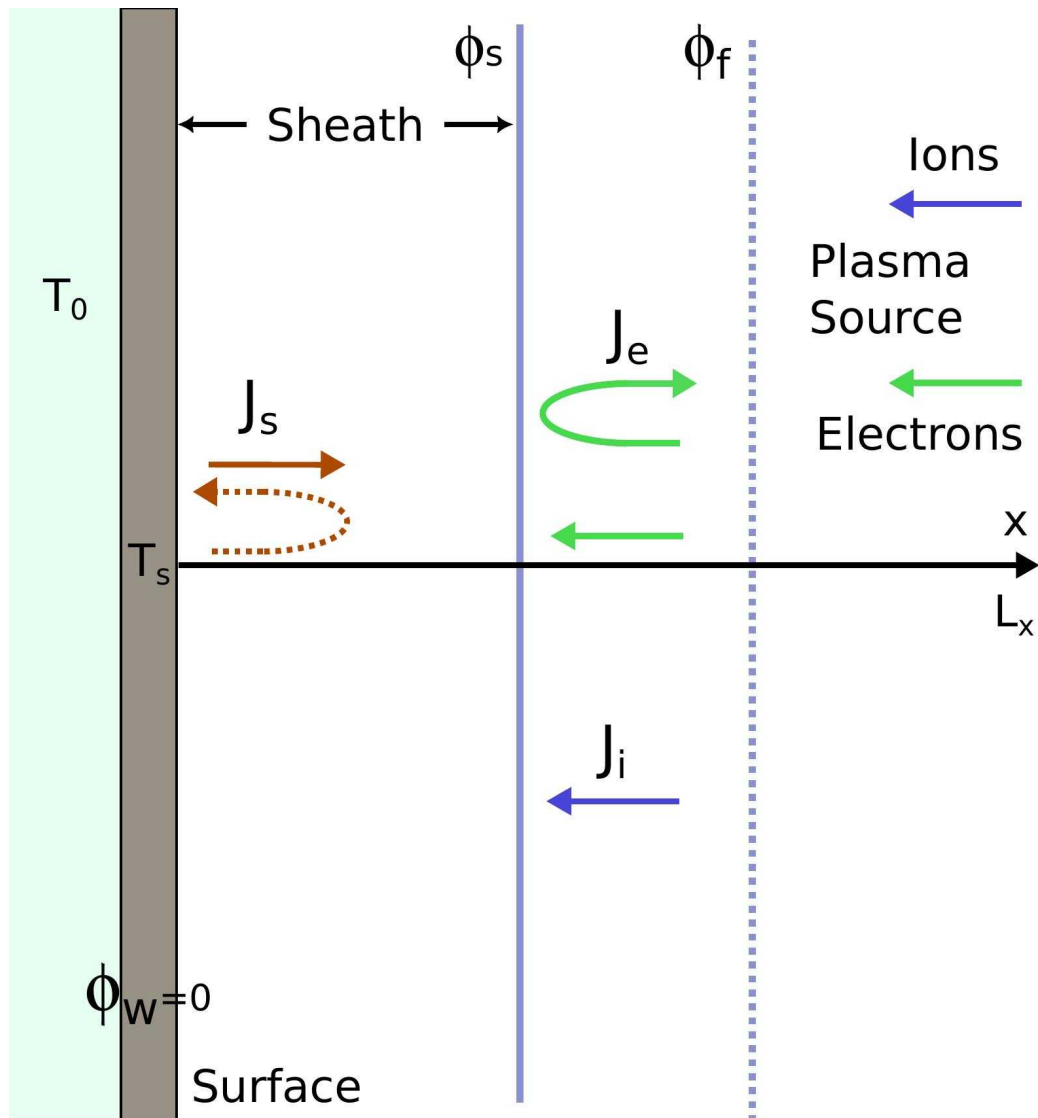
Fig. 2. The experimental results for tungsten plate in helium plasma. At  $t = 24$  min, corresponding to  $I_p = 98$  A,  $V_p = 190$  V,  $n_e \approx 4.0 \times 10^{18} \text{ m}^{-3}$

- \* Floating conditions
- \* Cooling of the plasma due to cold thermoelectrons
- \* Hysteresis

Physics of Plasmas 3, 281 (1996)



# Spot & Surface Model



\* Tungsten surface with  $\kappa$  in the range  $15-160 \text{ Wm}^{-1}\text{K}^{-1}$  (altered surface)

\* Fluid modeling and PIC simulations

\*  $L_x = 100\lambda_d$

\* Different plasma conditions, plasma source (**no electron cooling**),  $B=0$

→ Determine self-consistently  $T_s$

# Heat Flux & Fluid Approach of bifurcation

## Heat flux at the surface:

$$Q_c = \underbrace{J_s/e(2k_b T_s + B_w)}_{\text{Thermionic current surface cooling}} + \epsilon \sigma T_s^4 + \underbrace{\frac{K}{t}(T_s - T_0)}_{\text{Conduction}}$$

$$Q_p = \underbrace{J_i/e(2k_b T_i + E_i - B_w + e\phi_s)}_{\text{Ion heating}} + \underbrace{J_e/e(2k_b T_e + B_w)}_{\text{Electron heating}}$$

The constants of W are  
 $A = 0.6 \times 10^6 \text{ Am}^{-2}\text{K}^{-2}$ ,  
 $B_w = 4.55\text{eV}$  and  $\epsilon = 0.25$

Tokar, Nedospasov, and Yarochkin, Nuclear Fusion 32, 15 (1992)

## Currents:

$$J_s = A T_s^2 \exp\left(-\frac{B_w}{k_b T_s}\right) \rightarrow \text{Richardson Formula}$$

$$J_e = \frac{en_s c_e}{4} \exp\left(-\frac{e\phi_s}{k_b T_e}\right) \rightarrow \text{Maxwellian flux}$$

$$J_i = en_s c_s \rightarrow \text{Bohm flux}$$

## Sheath potential:

$$e\phi_s = e\phi_f - k_b T_e \log\left(1 + \frac{J_s}{en_s c_s}\right)$$

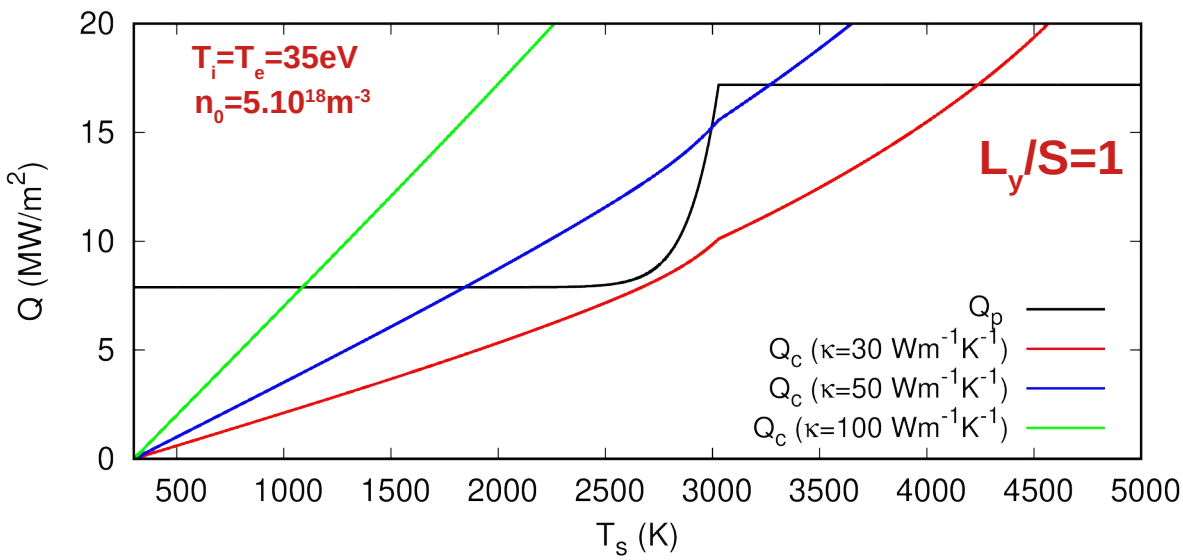
$\rightarrow$  1d Approx. ambipolarity  $J_i + J_s \simeq J_e$

## Surface Electric field:

$$E_s = f(\phi_s, J_s) \rightarrow \text{Until } E_s = 0 \text{ then SCL regime}$$

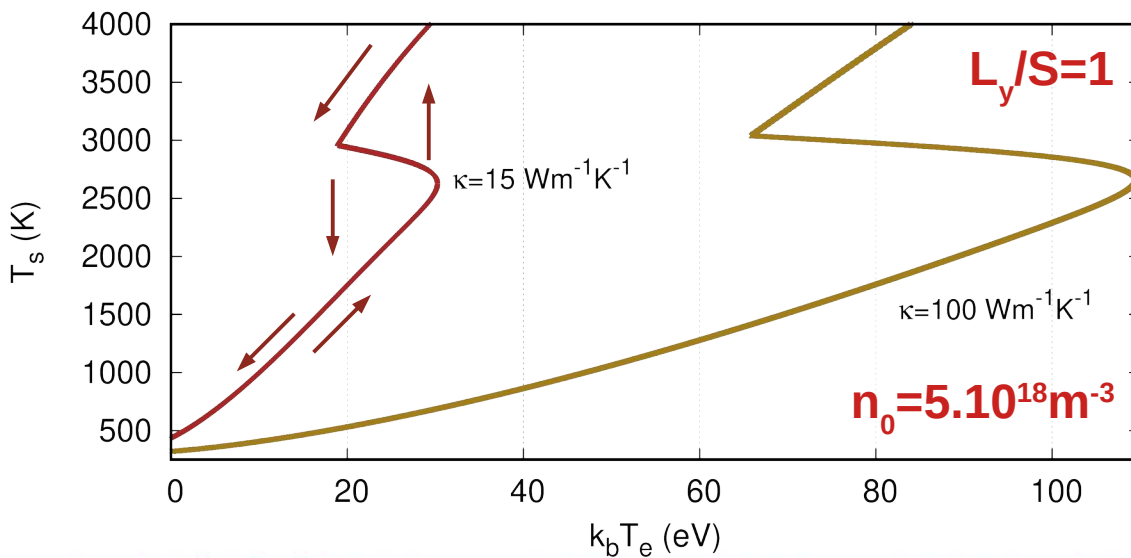
Hobbs and Wesson, Plasma Physics 9, 85 (1967)

# Heat Flux & Fluid Approach of bifurcation



\* Using fluid formula calculation of  $Q_p(t)$  and  $Q_c(t) \rightarrow T_s$

\* "S" curves of  $T_s = f(T_e, \kappa, n_0 \dots)$



\* Hysteresis arises from such characteristics  $\rightarrow$  bifurcation from a cold to a hot cathode surface and reciprocally

# Plasma Space potential vs. thermal cond.

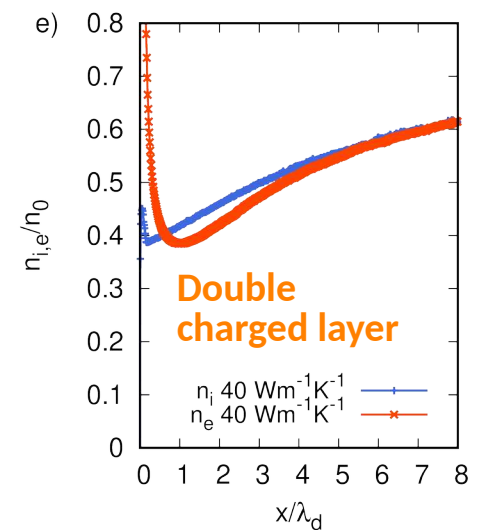
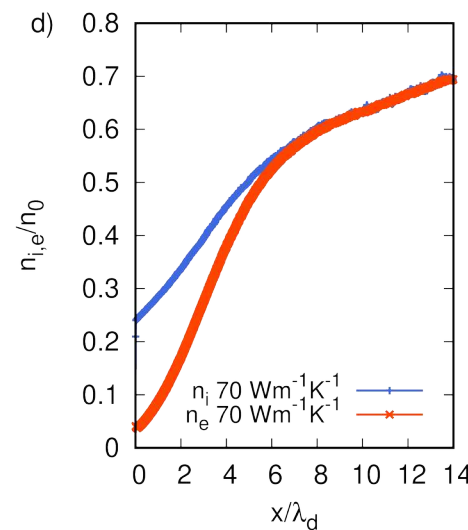
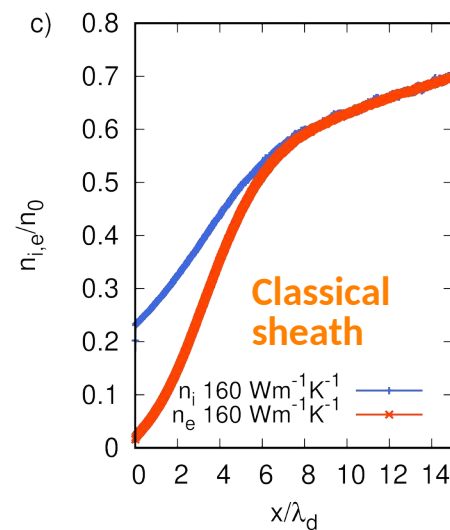
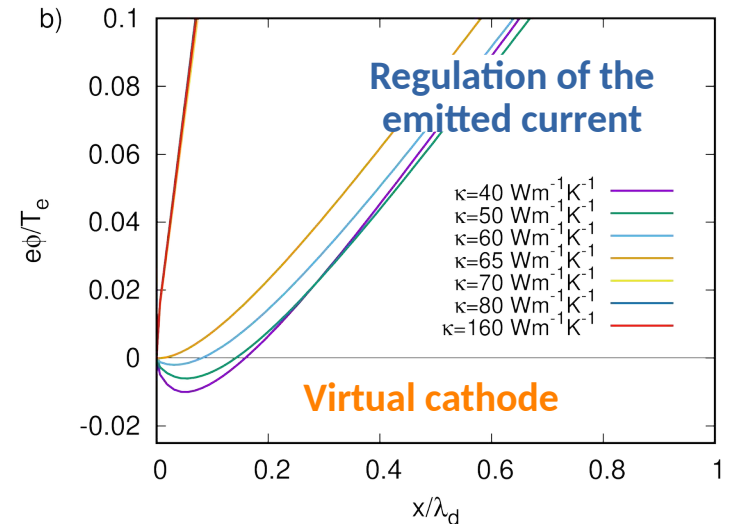
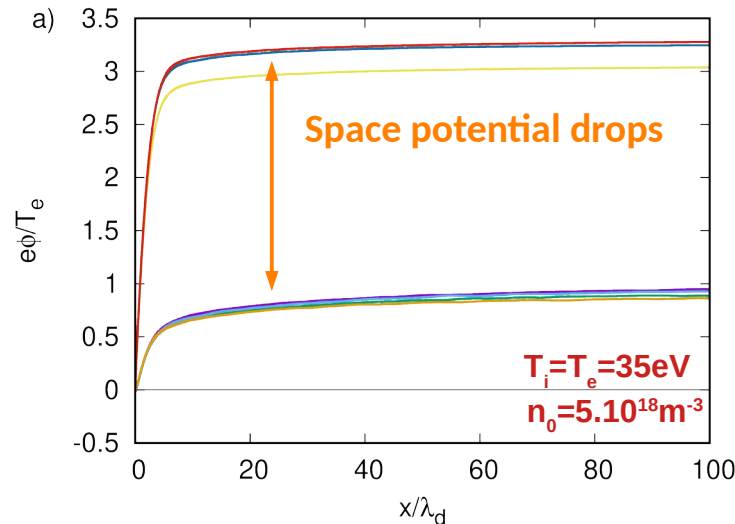
## w/ PIC simulations:

✱ At each  $t$ ,  $Q_p = Q_c \rightarrow T_s$   
until the steady state

✱ One parameter change  
( $T_e, \kappa, n_0$ ) = one  
simulation = one  $T_s$ , space  
potential...

✱ Averaging for several  
dozen of pl. periods for  
determining  $T_s$

✱ Hysteresis ?





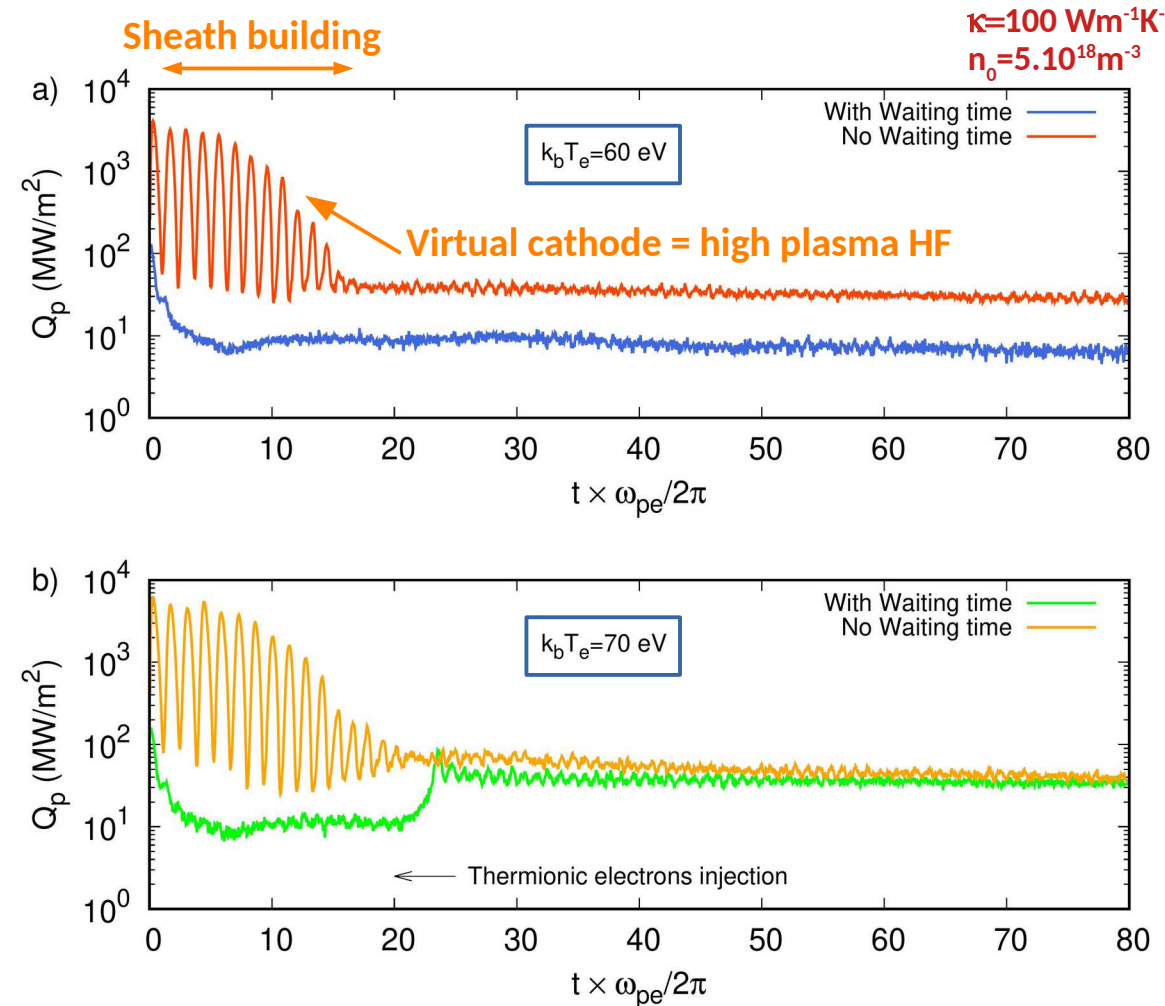
# PIC : Sheath building

\* At each  $t$ ,  $Q_p = Q_c$

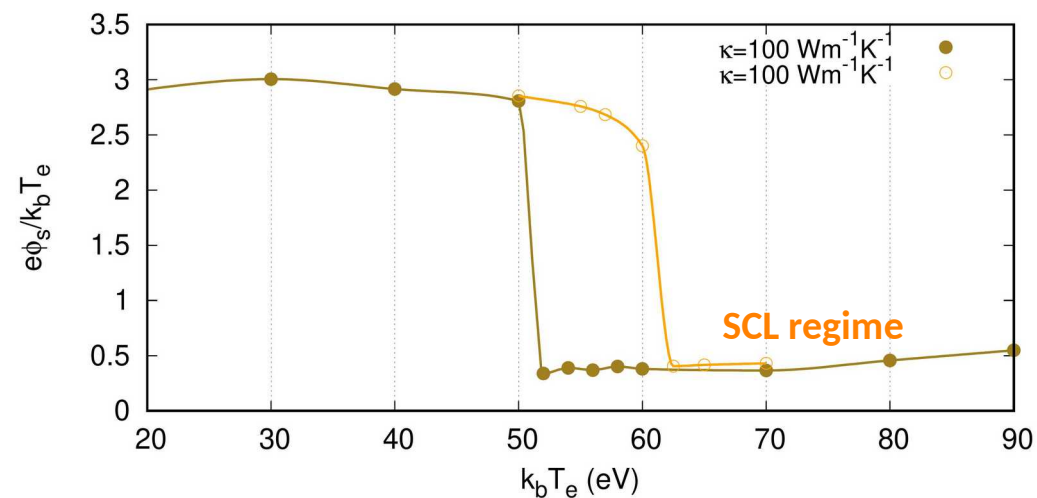
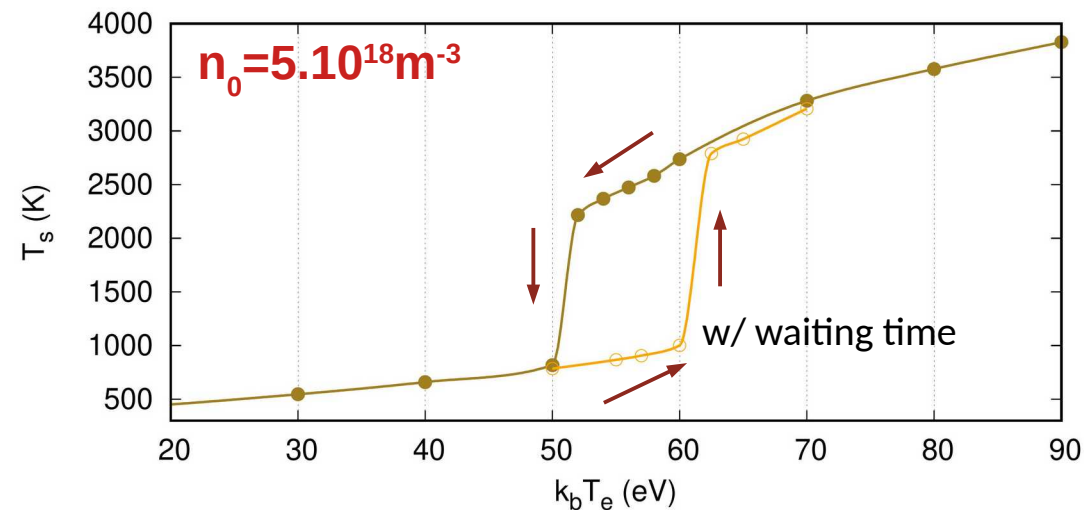
\* First plasma periods = sheath building and high heat loads

\* Introduction of a waiting time in the simulations before injecting TE electrons

\* For intermediate plasma heat loads can result in 2 different final states = hysteresis



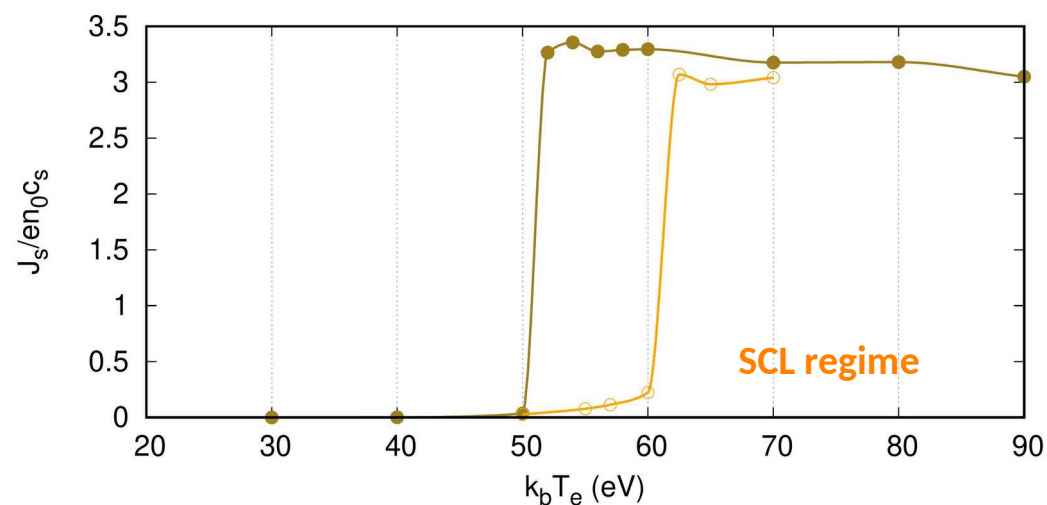
# PIC & Hysteresis



\* High  $V_f$ , low  $T_s$  and low current / low  $V_f$ , high  $T_s$  and max current

\* Hysteresis evidenced by changing initial conditions in the PIC simulations.

\*  $J_s$  saturates around  $3n_0 c_s =$  when emitted current  $\rightarrow$  Bohm current = bifurcation



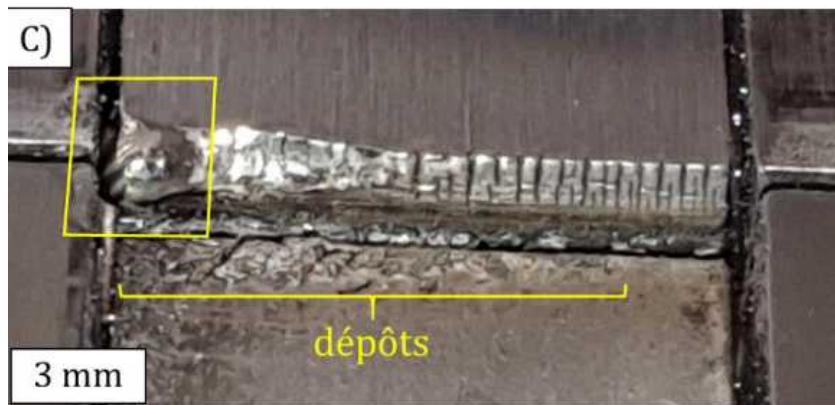
# B) Erosion & redeposition of a liquid metal plasma-facing components

Romain Avril, PhD

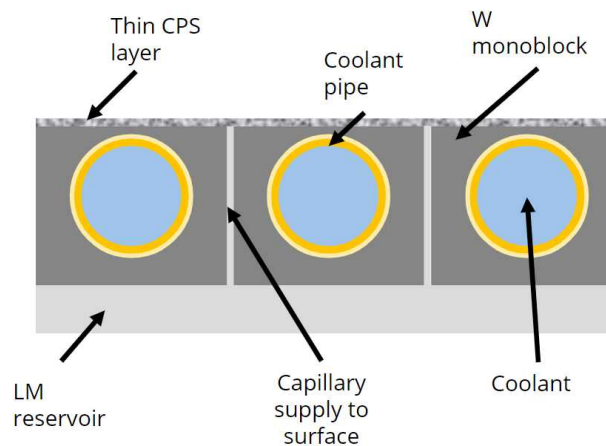
→ “Erosion and transport of lithium from a liquid metal wall facing a fusion plasma” - Romain Avril, Oral presentation at the “*Journée de la Matière Condensée 2024*”, 28-31 Oct. 2024, Marseille

# Liquid metal plasma-facing components

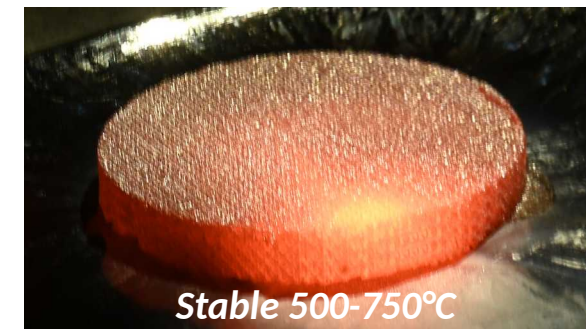
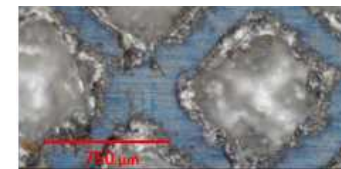
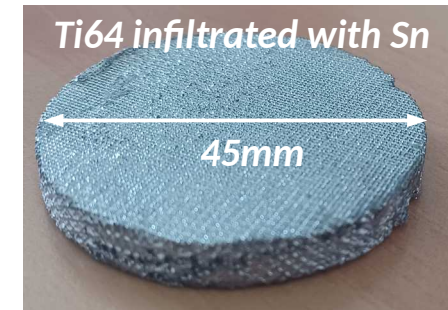
- Liquid metals might be an interesting option for economically competitive fusion reactors, especially for compact machines, due to 'self-healing' properties
- Several designs classified as function of the dominating heat transfer mechanism and flow characteristics (velocity, thickness, etc)



W Solid PFC = cracking / melting  
(Q. Tichit / IRFM thesis 2024)

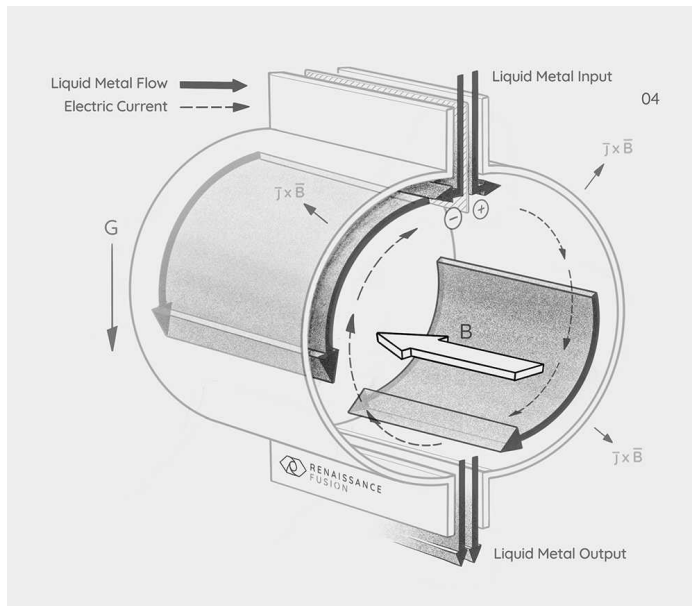


CPS working principle  
(Courtesy to T. Morgan 2023)

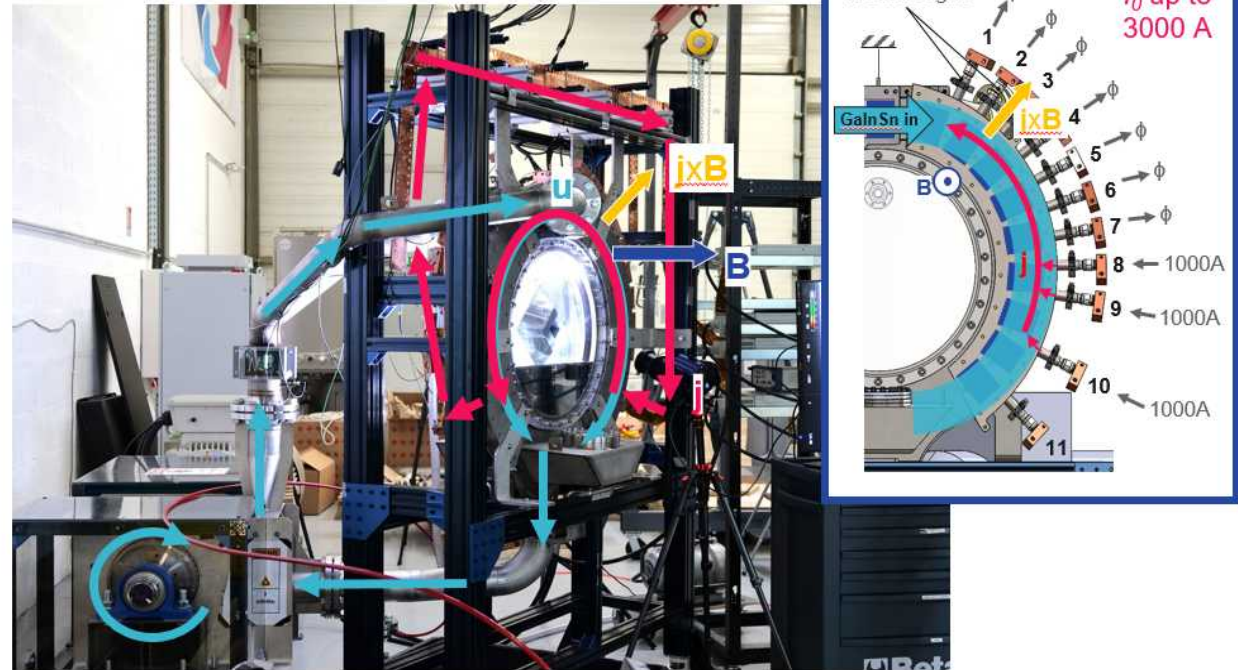


# Renaissance Fusion's concept of LMW

- 30cm thick fast flowing Li-LiH mixture with Pb ceramic pebbles between 700°C and 900°C
- Poloidal electric current (few kA) injected in the liquid metal layer + axial magnetic field (10T) = Radial force



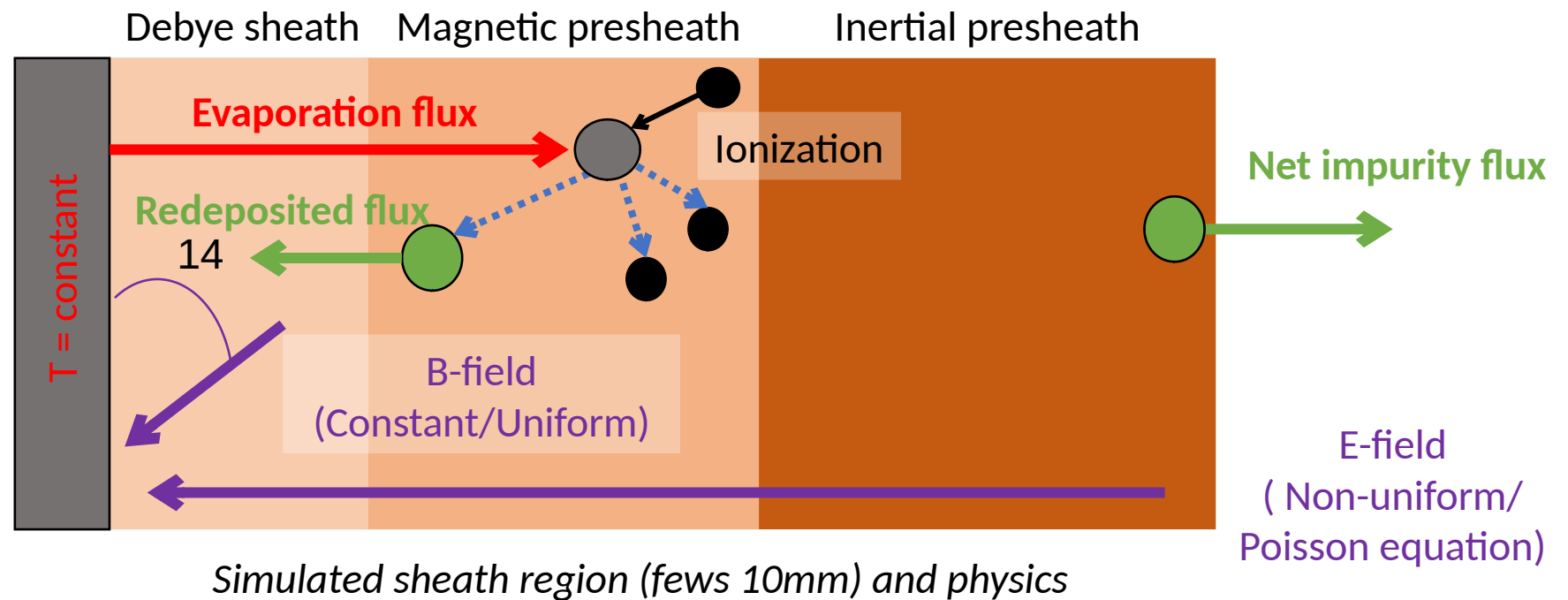
## 10 L/s meter-size GalnSn loop



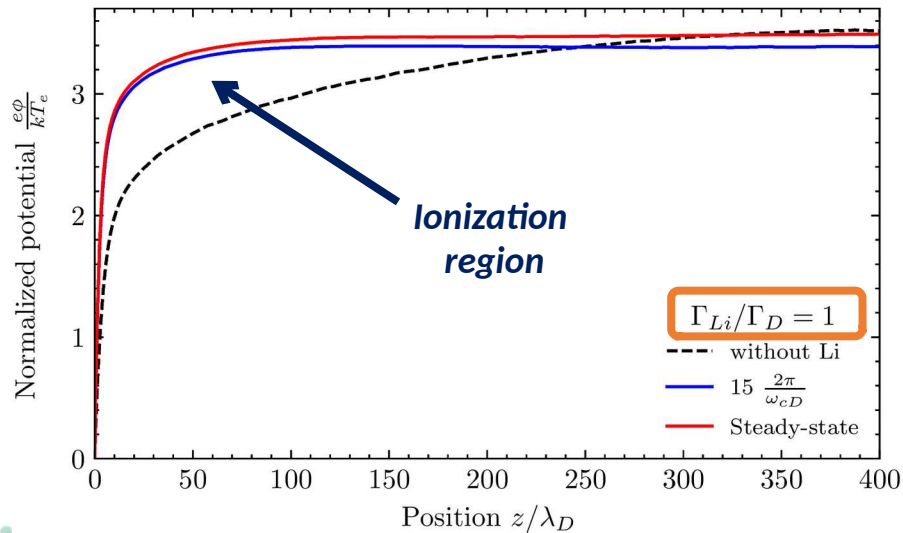
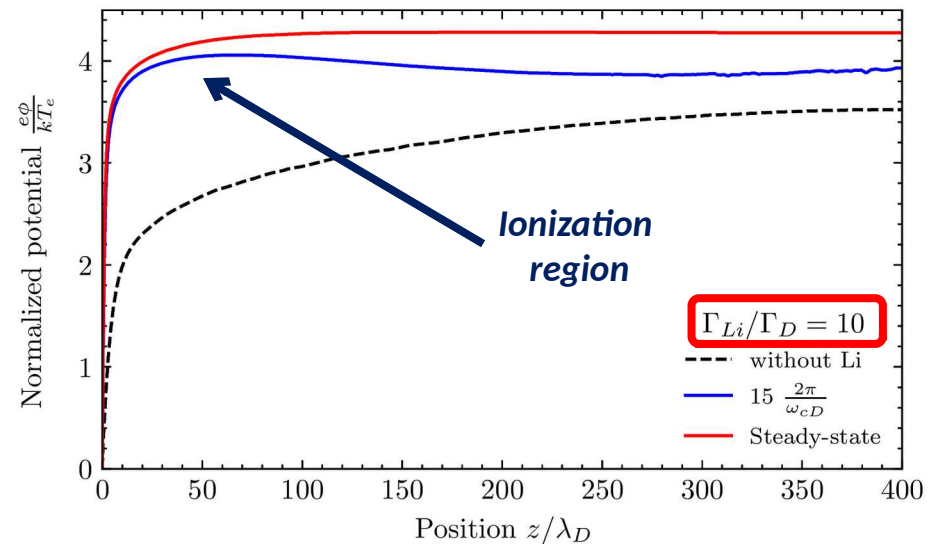
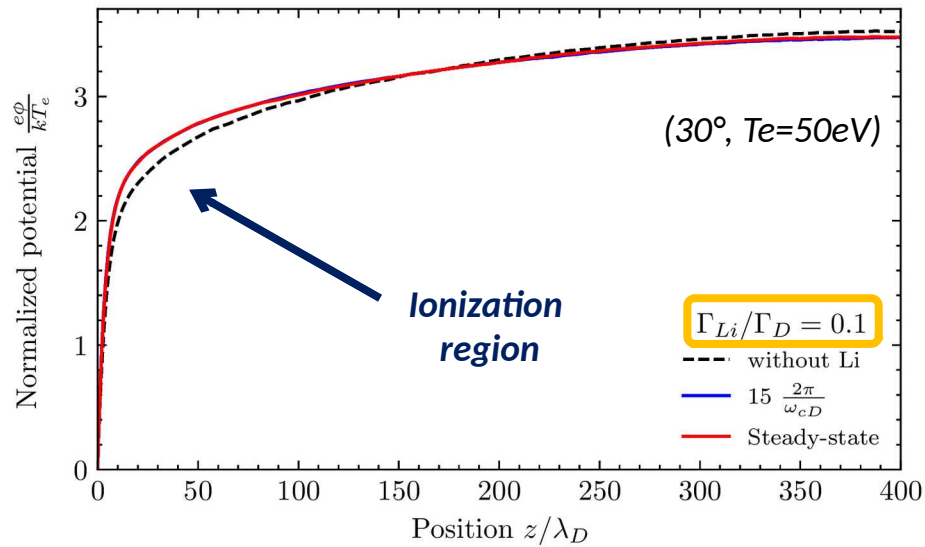
Skyfall liquid metal (galinstan) loop (taken from N. Baker-Wolff - 13th PAMIR conference)

# PIC model for ionization

- Investigation with a 1D3V Particle-in-Cell (PIC) code
- Electron-induced ionization is the only simulated atomic process
- Only evaporation is considered in the relevant temperature range where it is dominant (500°C-700°C)
- Surface temperature is constant (Renaissance Fusion's configuration)
- **Objective** : Make first redeposition estimations and investigate the impact of Li on sheath/presheath



# Space Potential profiles with Li



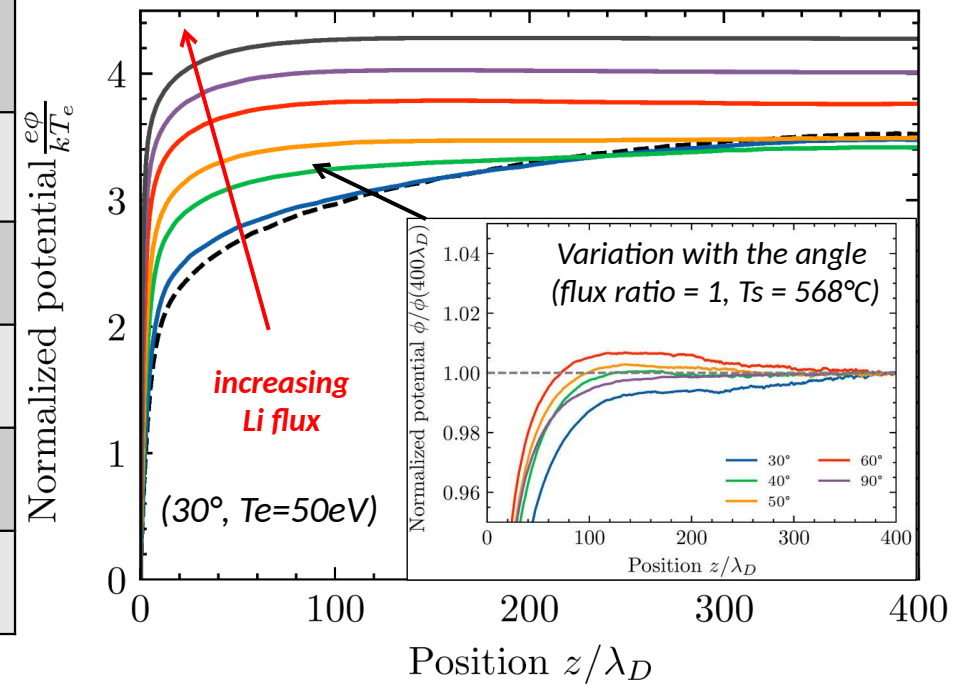
Evolution of the potential profile for several flux ratios

- Ionization in the presheath
- Potential profile flattening in the ionization region due to Li injection
- Decrease of the redeposition
- Transient potential hump

# Redeposition trends

- **4 keys parameters** :  $\Gamma_{\text{Li}}/\Gamma_{\text{D}}$ ,  $\lambda_{\text{iz}}/\lambda_{\text{D}}$ ,  $\theta$  and B
- High redeposition of evaporated Li atoms (>95%)
- Results in accordance with the work of *Brooks and Naujoks (2000)* made with BPHI-3D
- Prediction of a potential hump that accelerates Li ions towards the plasma (depends on the Li source and the magnetic inclination) => Reduces the redeposited fraction

Increased parameter	$\Gamma_{\text{Li}}/\Gamma_{\text{D}}$	$\lambda_{\text{iz}}/\lambda_{\text{D}}$	Redeposited fraction
(°C)	increases	increases	decreases
$n_0$ (m <sup>-3</sup> )	decreases	decreases	increases
$T_e=T_D$ (eV)	decreases	decreases	increases
B (T)	unchanged	unchanged	decreases
$\theta$ (deg)	unchanged	unchanged	depends

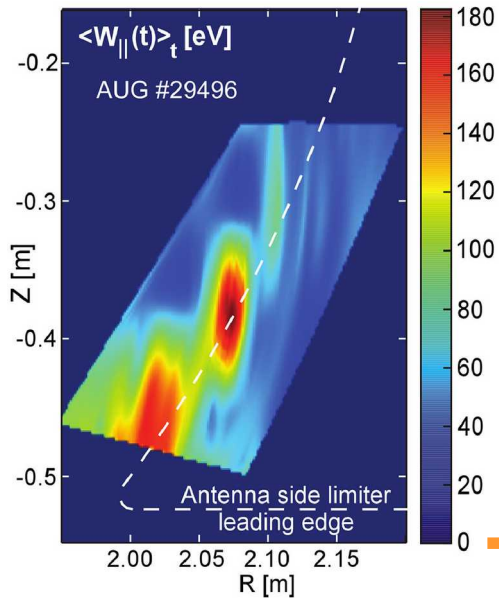




# C) Radio-frequency sheath and sputtering mitigation (ICRF antennas)

Léonel Tsowemoo, PhD

# Objectives & context (collab. IPP Garching + Uni. Basel)



180eV w/ ICRH vs.  
30eV Ohmic case  
(Bobkov NME 18,131)

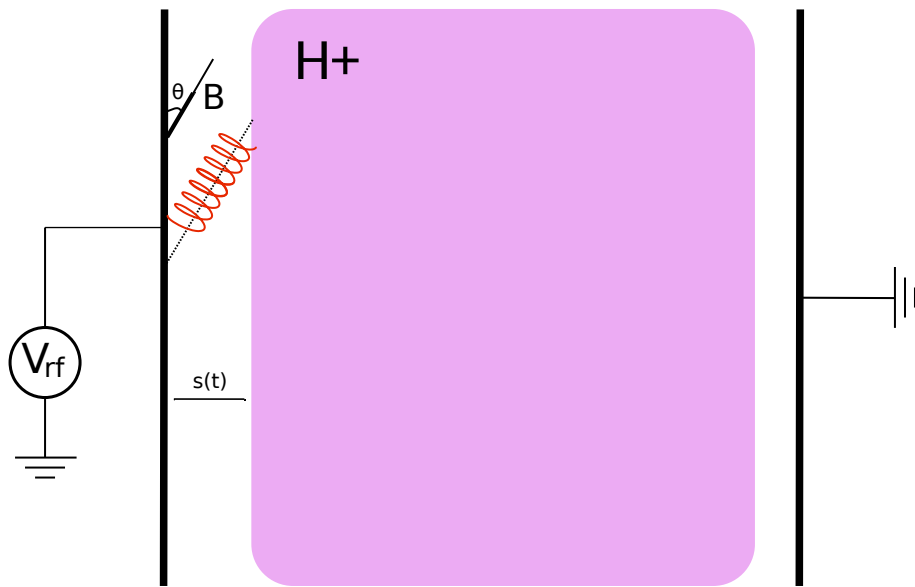
- \* ICRF antenna source of strong RF fields → oscillating sheaths
- \* Sheath rectification leads to ion acceleration → Sputtering
- \* Major concern for the application of ICRF power in a high-Z environment

## Objectives:

- Characterization of RF sheath properties for H/D/T species vs RF frequency, B amplitude and incidence (focus on grazing ones), sheath impedance + measurements @ Basel
- W sputtering due to C,O, B + self sputt. + redep. vs edge plasma properties + measurements @ Basel

# Model / some results

- 1D/3V symmetric RF plasma discharge
- Electrons magnetized ( $\rho < \lambda_d$ ) (not ions)



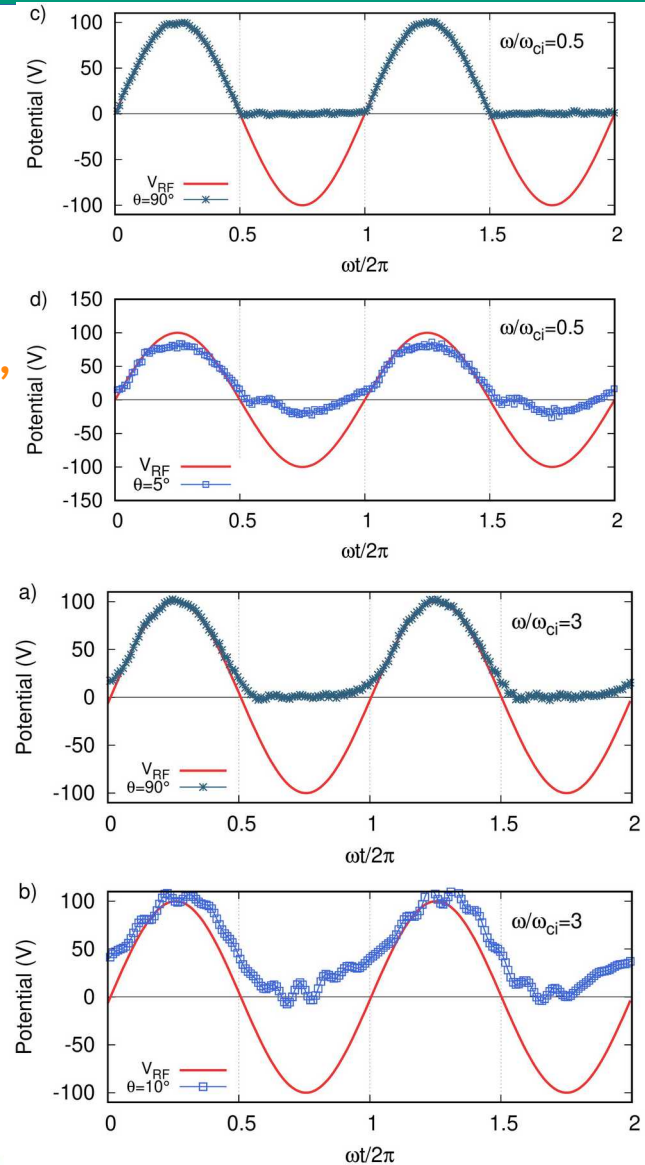
- \*  $n_0$  ranges  $10^{17}$ - $10^{19} \text{ m}^{-3}$  /  $T=2\text{eV}$  /  $V_{\text{rf}}=100\text{V}$
- \*  $\omega_{\text{rf}}$  scales with  $\omega_{\text{ci}}$

Low  $\omega$  & large  $\theta$ ,  
resistive sheath

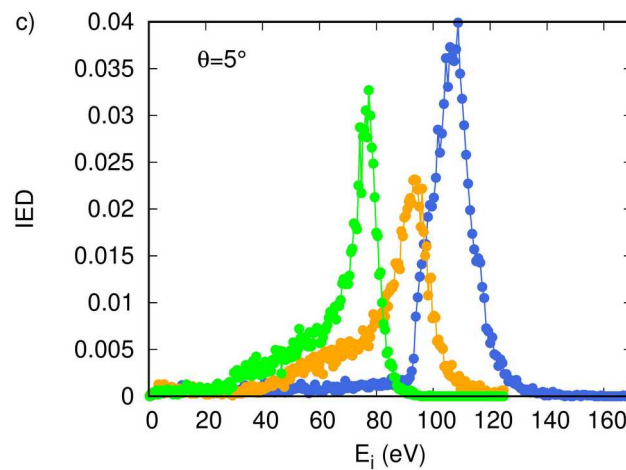
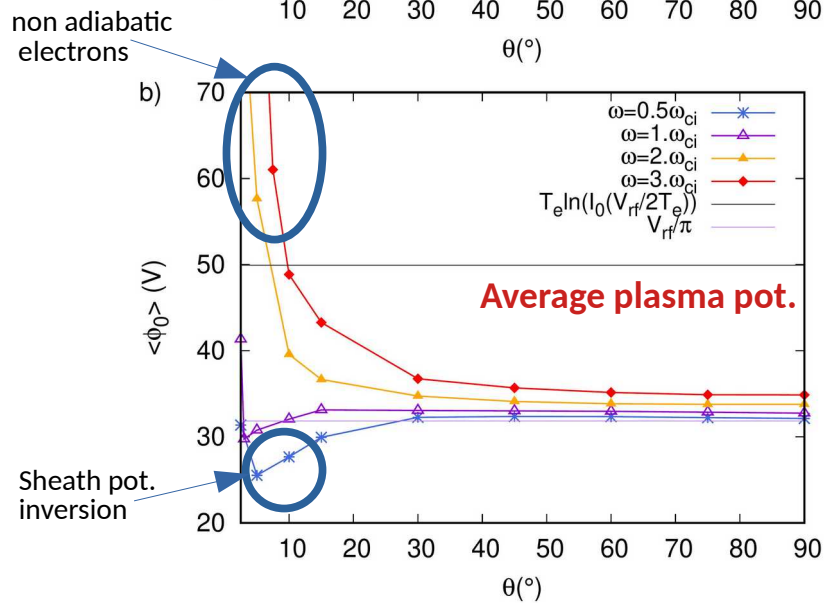
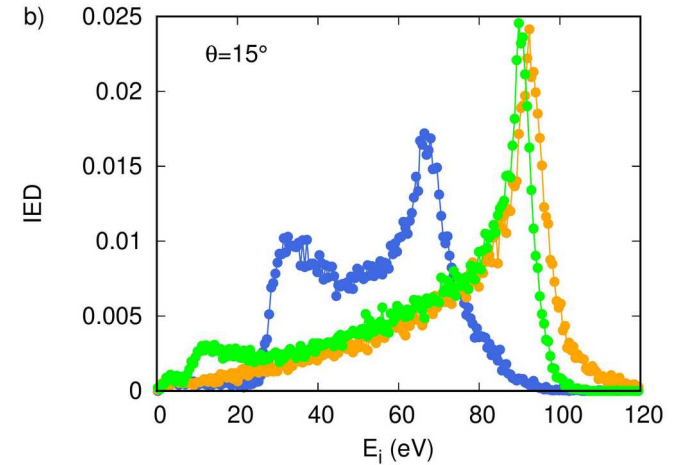
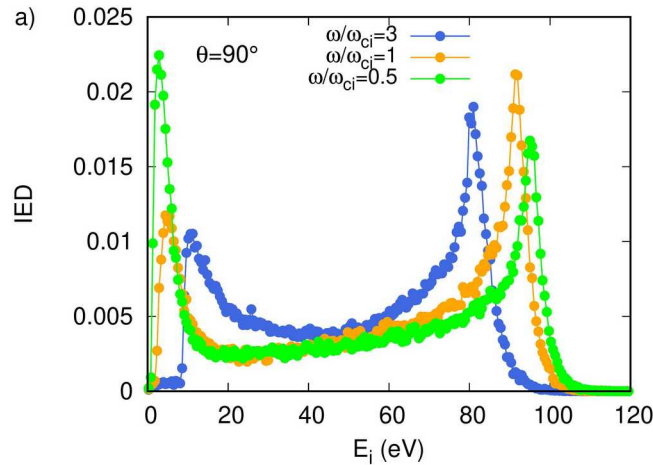
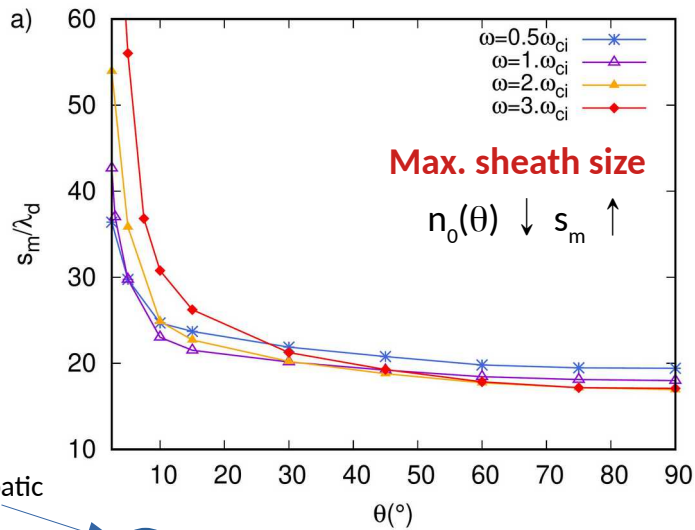
Low  $\omega$  & grazing  $\theta$ ,  
inverted sheath

Higher  $\omega$  &  
large  $\theta$ , less  
resistive sheath

Higher  $\omega$  & small  
 $\theta$ , capacitive  
sheath



# Model / some results



-  $\omega_{pi}/\omega_{rf} \downarrow$  with  $\theta \rightarrow$  ion dynamics

- IED&IAD influence the sputtering rate  $\rightarrow$  depends on both  $\omega$  and  $\theta$

- Adiabatic elec. approx. for rectified potential may fail at grazing incidence

- \* Diamond Open Access (free for both authors and readers)
- \* Hosted on the Episciences platform (CNRS / CCSD)
- \* Launched in 2024
- \* International editorial committee
- \* **SUBMIT!** (please)

